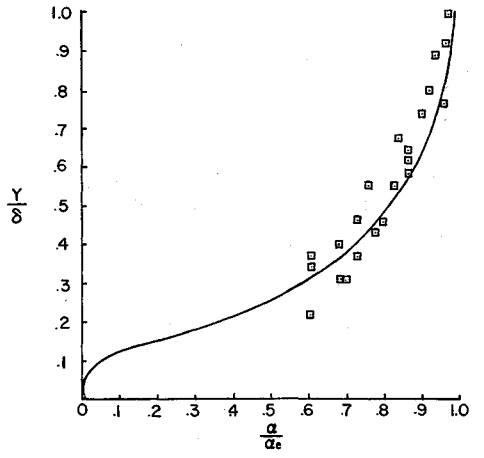

Fig. 3 Enthalpy profiles in the boundary layer (plotted points are experimental values).

The resulting equations for the equilibrium case are presented in Ref. 1 in the form of the familiar similarity variables. These require knowledge of the viscosity-density ratio and equilibrium Prandtl number in the boundary layer. In calculating the transport properties, the correlations given in Amdur and Mason[4] for a two-component mixture were used for viscosity and thermal conductivity. The viscosity and conductivity of helium was taken from Amdur and Mason.[4] The viscosity of argon was taken from Aeschliman[5] and Cambel.[6] The thermal conductivity of argon was taken from Ambur and Mason[4] below 5000°K and Knopp and Cambel[7] above 5000°K, The equilibrium specific heat was computed by an equation given by Cambel.[6]

The energy and momentum equations were put in integral form. The viscosity-density ratio and equilibrium Prandtl number were initially assumed unity. Then the momentum and energy equations were solved for the specific enthalpy distribution. The temperature, heavy particle density and electron density were determined from the Saha equation and the equation of state. Transport properties, viscosity-density ratio and the Prandtl number were computed and the process repeated until convergence.

Results

Figure 1 shows a typical variation of the equilibrium Prandtl number, Pr, and viscosity-density ratio, C, across the boundary layer. The ordinate on the boundary-layer plots is the dimensionless distance y/δ where δ is the boundary-layer thickness defined here to be the position where $h/h_e = 0.99$.

The results of Fig. 1 are interesting for two reasons. First, it is sometimes assumed that the viscosity-density ratio and equilibrium Prandtl number are equal to unity and constant across the boundary layer. This is clearly not the case. Secondly, it is apparently ionization that produces the abrupt changes in the properties.

Figures 2 and 3 show boundary-layer properties for a typical case. Experimental data are plotted with the theory. Curves for other properties show similar behavior. In all cases there is good agreement between the theory and the data, except close to the surface where frozen conditions may prevail. The unusual shape of the electron density profile in Fig. 3 is because of the cold wall. In the region where the data were taken, the temperature and density profile change very little compared to the other two profiles. Changes in enthalpy in Fig. 2 are therefore due to changes in electron density.

Conclusions

Assuming an equilibrium laminar boundary layer and using a form of local similarity theoretical property profiles agree favorable with the experimental data. Thus, it appears that the boundary layer in the recombination region behind primary shocks is laminar in nature and primarily in equilibrium, even at these high Mach numbers (~ 18) and with ionized gases. Boundary-layer studies behind shocks of this high strength have never been made. However, Hartunian et al.[8] indicated that perhaps the cool wall stabilized the boundary layer. They found for $T_w/T_e < 0.2$ the boundary layer was always laminar. Here $T_w/T_e = 0.02$, so this gives some credence to their statement. Very close to the surface there is perhaps a region where the flow is frozen.

The present interferometer was incapable of very close measurements. Further refinements in instrumentation are needed and should be carried out.

In addition, the effect of ionization has been shown on the viscosity-density ratio and the equilibrium Prandtl number. Previously, the temperature variations of transport properties for agon at one atmosphere have been computed (see, for example, Penski[9]). Here, and argon-helium mixture is considered and included in the boundary-layer theory.

References

[1] Mirels, H., "Laminar Boundary Layer Behind a Strong Shock Moving into Air," TN-D-291, 1961, NASA.

[2] Kemp, N. H. and Moh, T. C., "Laminar Boundary Layer Behind a Very Strong Shock Moving into Nitrogen," *Proceedings of the 5th International Shock Tube Symposium*. 1965, pp. 1013–1020.

[3] Besse, A. L. and Kelley, J. G., "Interferometer for Shock Tube," *Review of Scientific Instruments*, Vol. 37, 1966, pp. 1497–1499.

[4] Amdur, I. and Mason, E. A., "Properties of Gases at Very High Temperatures," *The Physics of Fluids*. Vol. 1, 1958, No. 5, pp. 370–383.

[5] Aeschliman, D. P., "An Experimental Determination of the Dynamic Viscosity of Atmospheric Argon from 3500 to 8500 Degrees Kelvin," NU-GDL Rept. B-1-68, March 1968, Northwestern Univ., Evanston, Ill.

[6] Cambel, A. B., *Plasma Physics and Magnetofluid Mechanics*, McGraw-Hill, New York, 1963.

[7] Knopp, C. F. and Cambel, A. B., "Experimental Determination of the Thermal Conductivity of Atmospheric Argon Plasma," *The Physics of Fluids*, Vol. 9, No. 5, 1966, pp. 989–996.

[8] Hartunian, R. A., Russo, A. L., and Marrone, P. V., "Boundary Layer Transition and Heat Transfer in Shock Tubes," *Journal of the Acrospace Sciences*, Vol. 27, 1960, 00. 587–594.

[9] Penski, K., "Zustands- und Transportgrossen von Argon Plasma," *Chem. Ing-Techn.*, Vol. 34, 1962, pp. 84–87.

Use of an Infrared-Imaging Camera to Obtain Convective Heating Distributions

DALE L. COMPTON*
NASA Ames Research Center, Moffett Field, Calif.

As re-entry configurations become more sophisticated, the convective heating patterns on these configurations tend to become both more complex and more sensitive to freestream conditions. There is, therefore, a need to develop rapid and accurate wind-tunnel techniques to measure heating distributions. One such technique is described in the present Note. Its essence is the measurement of infrared emission from the surface of a wind-tunnel model as a function of time by means of an infrared-sensitive imaging camera. Prior calibration of the infrared camera relates the emission to the surface temperature of the model. The time history of the surface temperature can then be realted to the heating rate by standard techniques. The output

Received March 31, 1972.
Index categories: Re-Entry Vehicle Testing; Boundary Layers and Convective Heat Transfer—Laminar; Boundary Layers and Convective Heat Transfer—Turbulent.

* Research Scientist, Thermo and Gas-Dynamics Division. Associate Fellow AIAA.

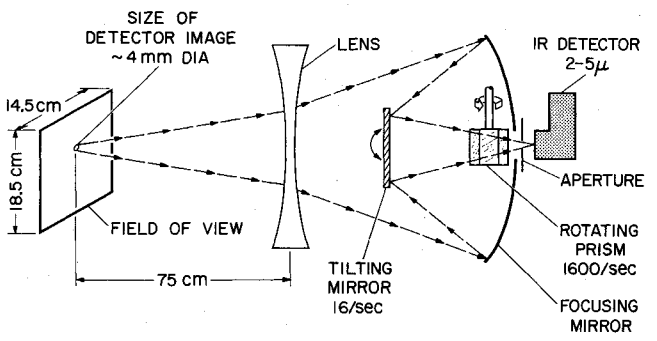

Fig. 1 Schematic drawing of camera optics.

of the camera is an electrical signal that is tape-recorded in analog form, then digitized and processed by computer, so that automated and relatively rapid data reduction can be accomplished. In addition, the camera produces real-time visual displays of the infrared emission as pictures on an oscilloscope screen. These pictures give immediate indications of hot and cool spots on the model.

The infrared-imaging camera is an AGA Corporation Thermovision, model 661. The infrared detector (indium antimonide, 2–5 μ spectral range) is focused on the field of view by means of a lens and two mirrors, as shown for a typical focal distance in Fig. 1. The image of the detector is swept through the field of view horizontally at a rate of about 1600 sweeps/sec by means of a rotating prism, and vertically at a rate of about 16 sweeps/sec by means of a tilting mirror. This produces 16 pictures/sec with about 83 lines in each picture since 17 of the horizontal line sweeps occur while the mirror is returning to its starting position at the top of the picture. As an alternative mode of operation, the motion of the tilting mirror can be stopped to give a line-scan mode in which the same line is swept repetitively 1600 times/sec.

As presently configured, the camera has an output signal-to-noise ratio of unity for a temperature change of about 2°C when the camera is viewing a blackbody near a temperature of 23°C. It has a maximum spatial resolution of about 55 elements/line, as determined by measuring the minimum distance between two signal sources such that the camera can detect that there are in fact two separate sources. Reference 1 gives both a more detailed description of the camera and a description of its initial use in measuring aerodynamic heating.

Calibration of the camera is performed by using an infrared energy source with surface-emissivity characteristics the same as those of the wind-tunnel model to be tested. Both source and model are sprayed with a high-emissivity flat-black paint, 3M Nextel. The paint thickness required is about 0.05 mm, and the resulting surface is slightly grainy in appearance. The paint stands up well under wind-tunnel tests and its thermal characteristics have proved unimportant insofar as obtaining heating rate is concerned for tests lasting more than about one second. Reference 2 gives more details on the calibration procedure.

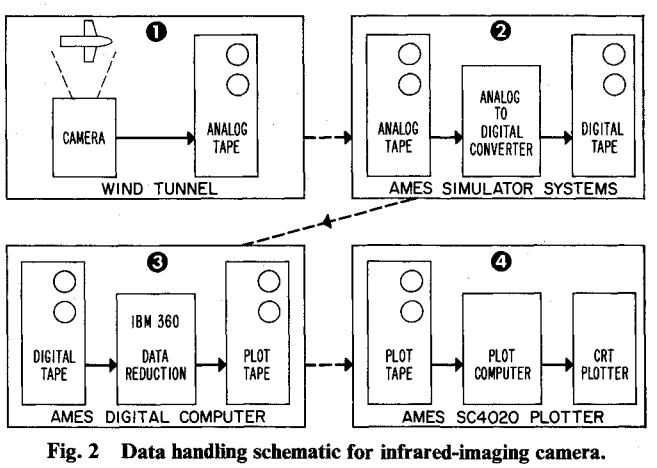

Fig. 2 Data handling schematic for infrared-imaging camera.

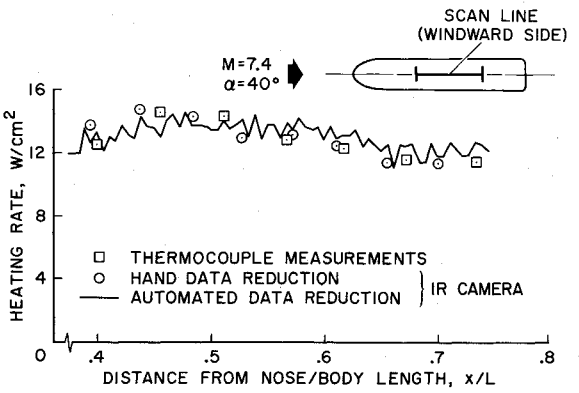

Fig. 3 Comparison of heating rates measured by means of thermocouples and an infrared-imaging camera.

An automated data-handling scheme has been developed to reduce the raw analog voltage data to heating rate distributions. The steps in the scheme are shown schematically in Fig. 2. The data are first recorded on analog tape. Then a digital tape suitable for use with standard digital computing equipment is produced from the analog tape. To produce this digital tape, the analog tape is replayed more slowly than it was recorded and the data are digitized continuously at a rate that produces 68 digital words along each scan line in the picture. This yields at least one digital point for each spatial resolution element. The amount of data produced is large, about 130,000 digital words/sec of wind-tunnel run time.

The digital tape is read by an IBM 360/67 computer, and computer routines have been written to organize the data so that standard heating-rate reduction can be accomplished. A heating-rate routine is available for thin-skin models; another for semi-infinite models is currently being written. Computation times have not become excessive—10 to 15 min/run are typical.

Contour plots of the heating-rate distribution are produced on an SC-4020 plotter. The outline of the model must then be superposed by hand on these plots.

Figure 3 shows a comparison between heating rates measured by means of both the infrared camera and thermocouples. The model in this test was a space-shuttle-orbiter body with a thin skin and the test was performed in the Ames 3.5-ft wind tunnel. The camera was used in the line-scan mode. Thermocouples were located beneath the skin of the model along the scan line. Two sets of measurements, labeled "automated data reduction" and "hand data reduction," are shown for the infrared camera. The former set was obtained by the automated procedure described in the preceding section. Each point of the digital data has been connected to the next by a straight line segment. The short-period fluctuations in these results are due primarily to noise introduced when the data were recorded on analog tape and when the data were digitized. At present, this noise probably limits the accuracy of the technique in measuring heat transfer to about $\pm 10\%$ at best. The measurements labeled "hand data reduction" were obtained by means of photographs taken of a direct oscilloscope display of the camera output. Both sets of infrared camera measurements are in good agreement with the thermocouple data.

The system has been used most frequently and with best success on models tested in the Ames 3.5-ft hypersonic wind tunnel, where run times are typically the order of a few seconds; hence, there are several tens of complete pictures per run. The wind-tunnel flow must not radiate in a spectral region in which the detector is sensitive, and the 3.5-ft wind tunnel satisfies this requirement.

Figure 4 shows data from a typical run. The model is the same as in Fig. 3. An unintentional single roughness element, just upstream of the field of view of the camera, has tripped the laminar boundary layer and caused a turbulent wedge with its higher attendant heating to form. This roughness element, caused by impact damage on a previous run, was small enough to

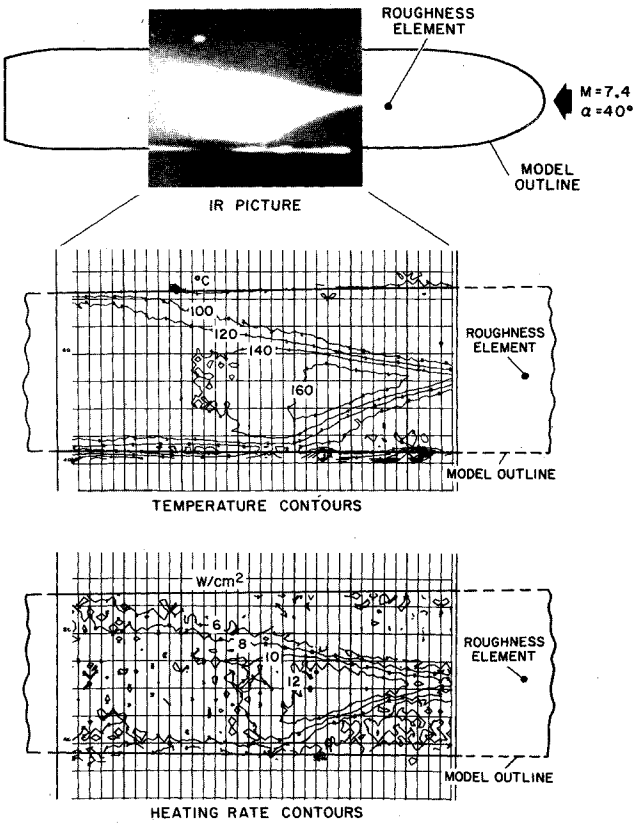

Fig. 4 Measurement of temperature and heating-rate distributions through a turbulent wedge by means of an infrared camera.

have easily escaped notice otherwise, since the model also had intentional roughness. Superposed on the outline of the model is a photograph of the viewing screen of the camera. Lighter regions have higher temperatures, and the turbulent wedge stands out clearly. The hot regions on the sides of the model are produced by pieces of tape. The lower two parts of the figure show computer-generated temperature and heat-transfer plots from this run. The turbulent wedge is evident in both of these plots.

In conclusion, the use of an infrared-imaging comera to obtain heating-rate distributions on complex aerodynamic shapes offers the opportunity to decrease data reduction time substantially with an accuracy in the data that is acceptable for most situations. Compared with thermocouples, the infrared camera offers the advantage that detailed heating-rate distributions can be more readily obtained. Compared with phase-change paint,[3] the problems of data handling for the camera are more amenable to automation since the camera output is directly in the form of voltage; thus, there are no photographic records to read. Furthermore, the camera can give the time history of heating rate, whereas phase-change paint can give only the time-averaged rate up to the time of phase change. This can be important if, as sometimes happens, transition on the model moves substantially during the test.

References

[1] Thomann, H. and Frisk, R., "Measurement of Heat Transfer with an Infrared Camera," *International Journal of Heat and Mass Transfer*, Vol. 11, 1968, pp. 819–826.

[2] Compton, D. L., "Convective Heating Measurement by Means of an Infrared Camera," TM X-2509, Feb. 1972, NASA.

[3] Jones, R. A. and Hunt, J. L., "Use of Fusible Temperature Indicators for Obtaining Quantitative Aerodynamic Heat-Transfer Data," TR R-230, Sept. 1965, NASA.

Observation of Ultraviolet Radiation from a Rocket Exhaust Plume at High Altitudes

A. W. MANTZ* AND J. J. LANGE†
Air Force Avionics Laboratory, Wright-Patterson Air Force Base, Ohio
AND
E. S. FISHBURNE,‡ D. C. MOYER,§ C. R. WATERS**
Grumman Aerospace Corp. Bethpage, N. Y.

DURING the past two years, several attempts have been made to observe vacuum ultraviolet radiation emitted from manmade events in space. The Orbiting Astronomical Observatory (OAO) –2, which was designed to observe the vacuum ultraviolet radiation from celestial bodies, was considered to be a system that could be used for these observations.[1]

The OAO has an exceptionally stable platform and a very high pointing accuracy. In addition, the spectral photometers provide a wavelength coverage from 1000Å to 4000Å. The first attempt to obtain vacuum ultraviolet radiation from manmade events occurred during the flight of Apollo 13. The Smithsonian Astrophysical Observatory Celescope experiment instruments at one end of the OAO were employed to obtain uvicon photographs of the liquid oxygen dumped from the Saturn SIVB stage after translunar injection. We were interested in the effects of solar radiation on the LOX dump that was continuously illuminated by the sun. This experiment did not produce a positive indication that the observation was successful.

The next event that was considered involved the release of barium at very high altitudes. It was felt that information concerning the vacuum ultraviolet emission from the barium cloud would aid considerably in the understanding of the various radiation processes involved, including the effects of solar raradiation and interaction with the earth's atmosphere at high altitudes. However, a careful analysis indicated that the small field of view of the Wisconsin Experiment Package on OAO-2, 10 min of arc, was too restrictive considering the uncertainties of the exact time of release of the barium cloud and the exact altitude and position of the cloud. This study led us to consider events that involved less positional error. After careful consideration, it was conjectured that the best observational conditions involved the exhaust plume of a rocket system already in orbit or a system going into orbit.

Recently, an observation of the exhaust plume of a rocket engine was made. Because of the nature of the OAO trajectory and the missile trajectory of the target vehicle, we were able to view the exhaust plume only for about 4 sec. During this time measurements were obtained in the 2980Å, 2380Å, 1920Å, and 1500Å spectral regions. The characteristics of these photometers are given in Table 1 together with the peak irradiance values. The actual data in digital counts are shown in Fig. 1. The digital

Received March 31, 1972. This research has been supported in part by Air Force Project 7660 at AFAL. Contractual support by the AFCRL Optical Physics Laboratory is gratefully acknowledged. This research was accomplished under the auspices of AFCRL contract 19628-71-C-0129. We wish to express our appreciation to Goddard Space Flight Center, The University of Wisconsin, and especially to T. Houck for making the OAO available and for their assistance during these measurements.

Index categories: Combustion in Heterogeneous Media; Solid and Hybrid Rocket Engines; Rarefied Flows.

* Chief Scientist/Surveillance Branch, Air Force Avionics Laboratory.
† Physisist, Air Force Avionics Laboratory.
‡ Research Section Head.
§ Project Engineer.
** Systems Engineer.